

Of course, a type of reaction other than compound-nucleus formation might exhibit such an energy dependence. The shape of the 10.5-Mev angular distribution has been fitted quite well¹⁷ with the Butler theory¹⁸ and with a radius $r=4.3\times 10^{-13}$ cm. The angular distributions measured here exhibit forward peaks characteristic of stripping, but there is no detailed agreement. Two illustrations of this are given in Fig. 2 for the 5.79-Mev data. The Butler curve for $r=2.5\times 10^{-13}$ cm fits the forward peak but not the slight (believed real) peak $\sim 70^\circ$. With $r=4.3\times 10^{-13}$ cm, the same radius that fits the 10.5-Mev data so well, there is a peak $\sim 70^\circ$,

¹⁷ S. T. Butler and J. L. Symonds, Phys. Rev. **83**, 858 (1951).

¹⁸ S. T. Butler, Proc. Roy. Soc. (London) **A208**, 559 (1951).

but for the most part the curve bears little resemblance to the data.

Extension of these measurements to higher energies, especially including the deuteron scattering, would help to clarify the interpretation.

ACKNOWLEDGMENTS

To the following people we are grateful and should like to extend our thanks for help in this experiment: J. K. Bair, H. O. Cohn, J. D. Kington, and H. B. Willard for advice and help in operating the generator; C. E. Melton for performing mass-spectrographic analyses of the tritium; S. J. Bame, Jr., and J. E. Perry, Jr., of Los Alamos for sending us their preliminary data prior to publication.

Photofission and Photoneutron Emission in Thorium and Uranium*

J. E. GINDLER AND J. R. HUIZENGA, *Argonne National Laboratory, Lemont, Illinois*

AND

R. A. SCHMITT, *University of Illinois, Urbana, Illinois*

(Received July 9, 1956)

Yield-energy relations have been determined radiochemically for the photofission and photoneutron reactions in Th²³² and U²³⁸. Excitation functions for the various reactions have been obtained by photon difference analyses of the corresponding yield functions. The photofission branching ratio for excitation energies of 8 to 11 Mev has been calculated to be approximately 0.08 for thorium and 0.2 for uranium. The relative photofissionability of thorium to uranium has been found to be about 2.3 times greater at betatron energies of 7 to 8 Mev than at 20 Mev. Also, evidence for bumps in the photofission excitation functions at about 6 Mev has been observed. Tentative explanations are presented for the relative photofissionability change and the bumps in the excitation functions. Characteristics of crude ($\gamma, 2n$) excitation functions are given for the two nuclides.

I. INTRODUCTION

EXCITATION functions for photofission and photoneutron emission in thorium and uranium have been reported previously.¹⁻⁸ Characteristics of these functions are given in Table I. Duffield and Huizenga⁴ also have reported that the fission branching ratio $\sigma_{(\gamma, f)}/[\sigma_{(\gamma, f)} + \sigma_{(\gamma, n)}]$ for uranium remains nearly constant, having an approximate value of 0.2 for photon

energies of 8 to 11 Mev. This is in agreement with later work⁶ in which the total neutron yields and fission yields for both thorium and uranium were measured. Since, for Th²³² and U²³⁸ nuclei excited to less than 11 Mev, the total neutron yield is composed of neutrons from the (γ, n) and (γ, f) reactions, the fission branching ratios were calculated from the total neutron and fission cross sections, assuming an average number of neutrons emitted per fissioning nucleus. These branching ratios together with those calculated from the excitation functions of reference 4 are given in Table II.

In the present experiment we have determined radiochemically the (γ, n) and (γ, F) yields for thorium and uranium produced by bremsstrahlung from the University of Illinois 22-Mev betatron. [We use (γ, F) to denote all processes initiated by a photon in which fission occurs. Mathematically, the cross section for the (γ, F) process may be represented adequately by $\sigma_{(\gamma, F)} = \sigma_{(\gamma, f)} + \sigma_{(\gamma, nf)} + \sigma_{(\gamma, 2nf)} + \dots$, since the emission of charged particles from heavy nuclides is small

* This work was supported by the joint program of the U. S. Atomic Energy Commission and the Office of Naval Research.

¹ G. C. Baldwin and G. S. Klaiber, Phys. Rev. **71**, 3 (1947).

² W. E. Ogle and J. McElhinney, Phys. Rev. **81**, 344 (1951).

³ R. E. Anderson and R. B. Duffield, Phys. Rev. **85**, 728 (1952); R. E. Anderson, B. S. thesis, University of Illinois, 1951 (unpublished).

⁴ R. B. Duffield and J. R. Huizenga, Phys. Rev. **89**, 1042 (1953).

⁵ Katz, Kavanagh, Cameron, Bailey, and Spinks, Phys. Rev. **99**, 98 (1955).

⁶ Lazareva, Gavrilov, Valuev, Zatsepina, and Stavinsky, *Conference of the Academy of Sciences of the U.S.S.R. on the Peaceful Uses of Atomic Energy*, July 1-5, 1955, Session of the Division of Physical and Mathematical Sciences (Consultants Bureau, New York, 1955), p. 217.

⁷ L. W. Jones and K. M. Terwilliger, Phys. Rev. **91**, 699 (1953).

⁸ R. Nathans and J. Halpern, Phys. Rev. **93**, 437 (1954).

TABLE I. Characteristics of photofission and neutron emission excitation functions for thorium and uranium.

Reaction	σ_{\max} (barns)	$E(\sigma_{\max})$ (Mev)	Half- width ^d (Mev)	$\int \sigma dE^f$ (Mev barns)	Ref- erence
$U^{238}(\gamma, F)^a$		16 ^e	5 ^e		g
$U^{238}(\gamma, F)$		15	8 ^e		h
$U^{238}(\gamma, F)$		14.6	6.8		i
$U^{238}(\gamma, F)$	0.18	14	7.6	1.2(0-20)	j
$U^{238}(\gamma, F)$	0.125	14	8.8	1.1(0-24)	k
$U^{238}(\gamma, F)$	0.20±0.03	14.0	6.7	1.71±0.14(0-28)	l
$Th^{232}(\gamma, F)$	0.051±0.007	14.1	7.0	0.64±0.06(0-28)	l
$U^{238}(\gamma, n)U^{237}$	0.53	11	3.6	2.6(0-20)	j
$U^{238}(\gamma, N)^b$		15.8	7.1		i
$U^{238}(\gamma, N)$	1.8	13	(5)	11.4(0-27.5)	m
$U^{238}(\gamma, N)$	0.96	14	6.4	7.1(0-25)	n
$U^{238}(\gamma, N)$	1.18±0.15	14.9	6.8	12.9±1.0(0-28)	l
$Th^{232}(\gamma, N)$	0.80±0.10	14.5	5.6	6.61±0.60(0-28)	l

^a (γ, F) indicates all processes initiated by a photon in which fission occurs.

^b (γ, N) indicates the total number of neutrons produced by the nuclear absorption of a photon. Because of the low probability of charged particle emission, the cross section for the (γ, N) process may be represented by

$$\sigma(\gamma, N) = \sigma(\gamma, n) + 2\sigma(\gamma, 2n) + 3\sigma(\gamma, 3n) + \dots + \bar{\nu}\sigma(\gamma, F),$$

where $\bar{\nu}$ represents the average number of neutrons produced by a gamma-excited nucleus which eventually fissions. These neutrons may be emitted before fission occurs, may be a result of the fission process, or may be a combination of the two.

^c Although the authors of reference 1 state that "no significance can be given to the shape of the curve of σ vs E ," the characteristics of their excitation function, given above, compare favorably with later analyses.

^d Half-width is defined as the full width at half σ_{\max} .

^e This value represents the half-width of the sigma₁ function of reference 2.

^f Integration limits in Mev are given in parentheses following the integrated value.

^g See reference 1.

^h See reference 5.

ⁱ See reference 2.

^j See reference 6.

^k See reference 3.

^l See reference 7.

^l See reference 4.

^m See reference 8.

compared to neutron emission and fission.^{9-12]} The (γ, n) yields were measured by isolating and counting the Th^{231} and U^{237} atoms formed; the fission yields, by separating and counting radioactive fission products. The cross sections for the (γ, F) and (γ, n) processes in thorium and uranium were determined by photon difference analyses of the corresponding yield curves.

II. EXPERIMENTAL

Simultaneous x-ray irradiations of thorium and uranium permitted the determination of the ratio of the (γ, n) to the (γ, F) yields for these elements under identical conditions. Absolute yields in terms of events per mole of element per 100 roentgens were computed by comparing the relative yields with the absolute (γ, F) yields of uranium. In addition to the conventional x-ray irradiations, several electron beam (probe) irradiations were made in order to determine the ratio of the (γ, F) to the (γ, n) yields of thorium and uranium at lower betatron energies. Details of the experiment are given below.

⁹ M. E. Toms and W. E. Stephens, Phys. Rev. **92**, 362 (1953).

¹⁰ M. E. Toms and W. E. Stephens, Phys. Rev. **98**, 626 (1955).

¹¹ E. V. Weinstock and J. Halpern, Phys. Rev. **94**, 1651 (1954).

¹² P. R. Byerly, Jr., and W. E. Stephens, Phys. Rev. **81**, 473 (1951).

Irradiations

Two types of external irradiations were made: simultaneous irradiations of thorium and uranium and individual irradiations of uranium. Simultaneous thorium and uranium irradiations were made at maximum bremsstrahlung energies of 8 to 20 Mev. Acid solutions containing five grams of uranyl nitrate hexahydrate or thorium nitrate tetrahydrate were placed in longitudinally separate halves of a thick-walled glass cylinder $1\frac{1}{2}$ inches in diameter and $1\frac{1}{2}$ inches in length. The cylinder was held in position next to the betatron doughnut by means of a Bakelite chamber. During periods of irradiation, this entire assembly was rotated by means of a small motor. In this manner, solutions of thorium and uranium received nearly the same integrated x-ray flux.

The number of photofission events per mole of uranium per 100 roentgens was determined for betatron energies of 8 to 20 Mev. The procedure consisted of irradiating 20 grams of finely crushed uranyl nitrate hexahydrate for 85 minutes. The uranium samples were wrapped in cadmium in order to eliminate thermal-neutron-induced fissions. The samples were 2.6 cm in diameter and were placed at a mean distance of 98 cm from the betatron target. Consequently, the angular variation of the incident x-rays was negligible. During an irradiation, fluctuations of the x-ray intensity were kept to a minimum. A thick-walled aluminum ionization chamber connected to a vibrating reed electrometer was used to monitor the x-ray beam. The ionization chamber was calibrated in roentgens for the betatron energy range of 8 to 20 Mev by comparing the electrometer reading with the average reading of two 100-r Victoreen thimbles placed at the center of an 8 cm×8 cm Lucite block. The absorption of 14-Mev bremsstrahlung by the uranium sample and its container was measured by counting the activities induced in thin copper disks placed in front of and behind the sample holder during irradiation. The measured x-ray intensities at all betatron energies were corrected for this absorption.

Reaction cross sections were calculated by the photon difference method.¹³ Corrections were made for the

TABLE II. Photofission branching ratios for thorium and uranium.

E (Mev)	U^{238} ^a	U^{238} ^b		Th^{232} ^b	
		$\bar{\nu}=2.5$	$\bar{\nu}=3$	$\bar{\nu}=2.5$	$\bar{\nu}=3$
6.5		0.24	0.27	>0.20	>0.22
7		0.24	0.28	0.18	0.20
8	0.25	0.22	0.24	0.14	0.15
9	0.21	0.19	0.21	0.10	0.11
10	0.16	0.23	0.26	0.08	0.08
11	0.18	0.23	0.26	0.08	0.08

^a See reference 4.

^b See reference 6.

¹³ L. Katz and A. G. W. Cameron, Can. J. Phys. **29**, 518 (1951). We are grateful to L. Katz for the low-energy supplement to the photon difference tables.

bremsstrahlung absorption by the Lucite block and for the comparative distances ($1/r^2$) of the sample and the beam monitor from the betatron target. The Ba^{139} fission product was separated from the irradiated uranium sample and counted in a calibrated counter⁴ to give the number of fissions produced in the sample. By appropriate calculations, the number of fissions per mole of uranium per 100 roentgens was then determined.

Although this method of determining the photofission yield of uranium is essentially the same as that reported in reference 4, it differs in one respect. In the present experiment, the uranium samples and the Lucite block containing the R thimbles were placed far enough from the betatron target to permit a uniform x-ray intensity across their surfaces. It has been observed that unless this condition of uniformity has been fulfilled, the $1/r^2$ distance correction for x-ray intensity no longer applies. It is felt that this is the main source of discrepancy between our uranium yields and those quoted in reference 4.

A series of probe irradiations was made with metallic bars of thorium and uranium, $\frac{1}{4}$ inch in diameter and $\frac{5}{8}$ inch in length, which served both as the x-ray generators and the x-ray targets. Such an irradiation setup is a modification of the conventional probe arrangement.¹⁴ The increased specific activity of samples irradiated in this manner over those irradiated in the external beam permitted the relative (γ, F) to (γ, n) yields to be extended to energies of 6, 7, and 8 Mev. In order to establish the difference between yields induced by probe irradiations and those induced by external irradiations, uranium samples were bombarded by both methods at betatron energies of 8 and 19.8 Mev. The ratios of (γ, F) to (γ, n) yields obtained from the internal irradiations agreed, within experimental error, with those obtained from external irradiations (see Fig. 1).

Radiochemical Procedures

1. Determination of Residual (γ, n) Atoms, Uranium-237 and Thorium-231

The procedure used for the determination of residual U^{237} atoms has been described previously.⁴ A fraction of each irradiated uranium sample was separated from its daughter activities and fission products by ether extraction. A known amount of this purified uranium was deposited as the oxide on platinum over a specified area and counted with a standard end-window Geiger counter. A 4.6-mg/cm² aluminum absorber was placed over the sample to eliminate any counts due to the alpha activity of the uranium. The counter had been previously calibrated for the absolute beta counting of U^{237} by counting weighed amounts of neutron-irradiated U^{236} and by comparing this counting rate with the Np^{237} alpha activity which resulted from the

¹⁴ R. A. Becker, Rev. Sci. Instr. 22, 773 (1951).

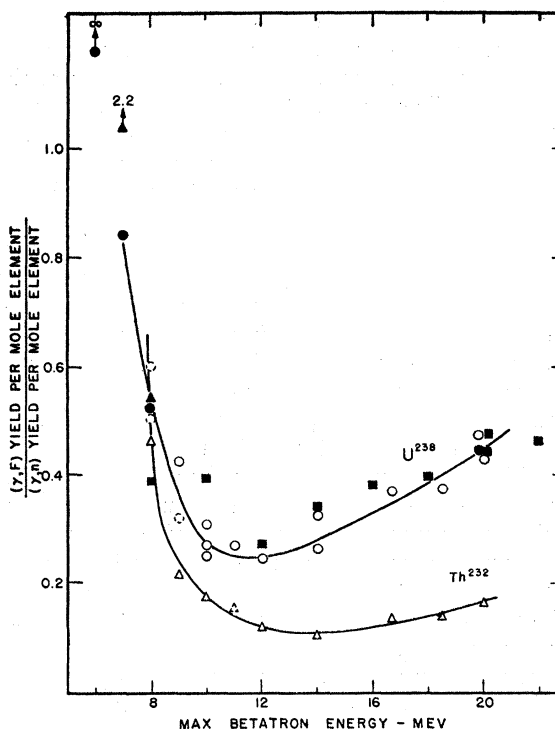


Fig. 1. Ratios of the total number of photofission events per mole element to the number of residual (γ, n) atoms per mole element as a function of maximum betatron energy. Uranium irradiations: \circ , x-ray, this work; \bullet , probe target, this work; \blacksquare , x-ray, reference 4. Thorium irradiations: \triangle , x-ray, this work; \blacktriangle , probe target, this work. The broken circles represent uranium data having errors of approximately $\pm 40\%$ because of low U^{237} counting rates. The broken triangle represents a weighing error of $\pm 25\%$ in the determination of the thorium fission yield.

decay of the U^{237} . By using this information together with the known half-lives of U^{237} and Np^{237} , the counting efficiency of the counter was calculated.

Blank runs were made in which nonirradiated uranium was subjected to the same chemistry and counting procedure as that described above. This was done in order to correct irradiated samples for the growth of uranium daughters and for an activity attributed to the alpha fine-structure in the decay of uranium isotopes. For the particular geometry of our counter, the growth rate per hour for the daughters of natural uranium was found to be 0.45 ± 0.05 counts per minute per milligram [(counts/min)/mg] U_3O_8 . The fine-structure counting rate was 1.1 ± 0.4 (counts/min)/mg U_3O_8 . Net counting rates for the U^{237} atoms varied from 0.4 to 150 (counts/min)/mg U_3O_8 .

The Th^{231} activity was determined in a manner similar to that used for the activity determination of U^{237} . Irradiated thorium was separated chemically from its daughters and fission products and deposited as the oxide on platinum. The Th^{231} activity was then measured with a Geiger counter.¹⁵ A 4.6-mg/cm²

¹⁵ Magnusson, Huizenga, Fields, Studier, and Duffield, Phys. Rev. 84, 166 (1951).

aluminum absorber was again used to eliminate counts due to thorium alpha activity. The Geiger counter was calibrated for the absolute beta counting of the Th^{231} in the following way. A sample of highly enriched U^{235} was separated chemically from its daughters and deposited as the oxide on platinum. The $(\text{U}^{235})_3\text{O}_8$ deposit was approximately equal in weight and area to that of subsequent thorium deposits. The growth of the beta activity in the sample was followed to equilibrium. By extrapolating the initial linear increase in the beta-growth rate back to the time of chemical separation of the uranium from its daughters, the counting rate associated with the U^{235} alpha fine-structure was determined. This amounted to 14% of the equilibrium beta-counting rate. The counter efficiency was calculated by subtracting the counting rate of U^{235} , as determined above, from the equilibrium counting rate and dividing this difference by the number of disintegrations per unit time of the U^{235} . The latter disintegration rate was determined from the weight of the U^{235} and its half-life.

Blanks were also run with nonirradiated thorium in order to determine the fine-structure counting rate and the beta-growth rate per hour due to thorium daughters. These background corrections amounted to 0.31 ± 0.02 (counts/min)/mg ThO_2 and 0.12 ± 0.04 (counts/min)/mg ThO_2 , respectively. Net counting rates for the Th^{231} atoms varied from 1.5 to 140 (counts/min)/mg ThO_2 .

2. Fission Determinations

The number of fissions occurring for each irradiated uranium sample was determined by measuring the number of Ba^{139} atoms produced. This was done by chemically separating the barium fission products from uranium¹⁶ and by counting them with a Geiger counter which had been previously calibrated.⁴ The calibration was performed by chemically separating and counting the barium fission products which resulted from a known number of slow-neutron-induced fissions of U^{235} . In calculating the total photofission yields, we have assumed that the photofission barium yield of U^{238} is 0.9 of the slow-neutron fission barium yield for U^{235} . This value is in agreement with experimental results.^{5,17-19}

Barium (139) was again isolated and counted with the calibrated Geiger counter in order to determine the number of fissions occurring in the thorium samples. It was assumed that the percentage yield of Ba^{139} produced by the photofission of thorium was the same as that produced by the photofission of natural uranium.

¹⁶ *Radiochemical Studies: The Fission Products* (McGraw-Hill Book Company, Inc., New York, 1951), National Nuclear Energy Series, Plutonium Project Record, Vol. 9, Div. IV.

¹⁷ R. A. Schmitt and N. Sugarman, *Phys. Rev.* **95**, 1260 (1954).

¹⁸ H. G. Richter and C. D. Coryell, *Phys. Rev.* **95**, 1550 (1954).

¹⁹ Glendenin, Steinberg, Inghram, and Hess, *Phys. Rev.* **84**, 860 (1951).

It is estimated that this assumption is valid within $\pm 10\%$.²⁰

Because of the relatively short-lived radium daughters of thorium which follow the chemistry of barium, precautions and corrections to data are required that are not necessary when uranium is the irradiated material. These radium daughters are responsible for a beta growth that is found in the presence of the decaying barium fission products separated from irradiated thorium. In order to reduce the amount of the radium isotopes present at the time of counting, thorium solutions which were to be irradiated in the external x-ray beam were treated chemically prior to the irradiation. This treatment consisted of adding a few drops of barium carrier to the thorium nitrate solution and precipitating the barium as the chloride. Two additional barium chloride precipitations insured the removal of radium. However, during the irradiation period, radium daughters grew in from the thorium until the time of chemical separation of the barium fission products. In order to determine the extent of this growth, blank runs were made in

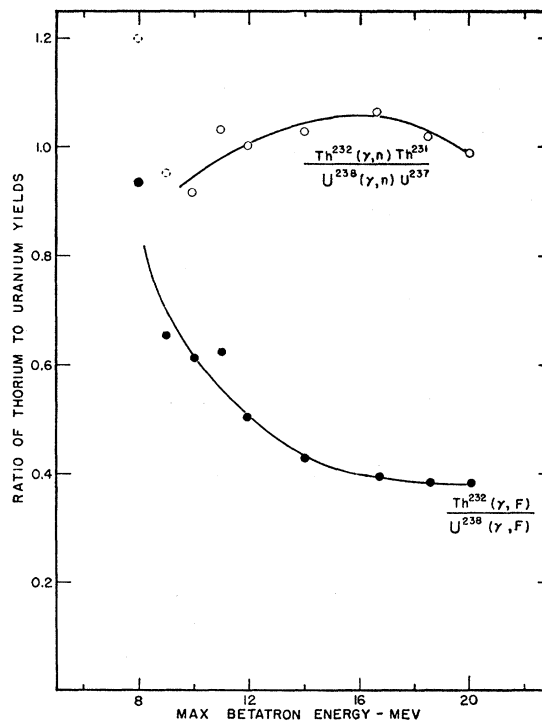


FIG. 2. Ratio of thorium to uranium yields as a function of maximum betatron energy. \circ , ratio of $\text{Th}^{232}(\gamma, n)\text{Th}^{231}$ events per mole of thorium per 100 r to $\text{U}^{238}(\gamma, n)\text{U}^{237}$ events per mole of uranium per 100 r. The broken circles represent data having large errors in the determination of the U^{237} activity (see Fig. 1). \bullet , ratio of photofissions per mole of thorium per 100 r to photofissions per mole of uranium per 100 r. The 11-Mev value may be in error by $\pm 25\%$ because of an error in weighing which affects the thorium fission determination (see Fig. 1).

²⁰ D. M. Hiller and D. S. Martin, Jr., *Phys. Rev.* **90**, 581 (1953), have reported a Ba^{140} yield of $6.6 \pm 0.5\%$ for the 69-Mev x-ray fission of thorium.

which nonirradiated thorium solutions were subjected to the same chemical treatment as the irradiated solutions. The beta-counting data for an irradiated sample were then corrected by using the information gained from the blank run.

Because of the chemical treatment of the thorium solutions with barium carrier prior to irradiation and the subsequent isolation of the barium fission products, any incomplete precipitation of the barium, initially added, would affect the chemical yield in the fission product analysis. For this reason, thorium solutions in which barium had been precipitated to remove radium daughters were analyzed for their barium content. It was found that there was sufficient barium carry-over to affect the final fission determination by approximately 5%. The final thorium results have been corrected for this error.

For thorium samples irradiated as probe targets, the chemical treatment described above was not possible. It was for this reason that the activity of I^{134} was measured only over the energy range, 6 to 8 Mev. An empirical relation between the Ba^{139} and I^{134} counting rates was established by direct measurement and this relation was then assumed to be independent of energy. The I^{134} activity was used to calculate the fissions over this energy range, 6 to 8 Mev.

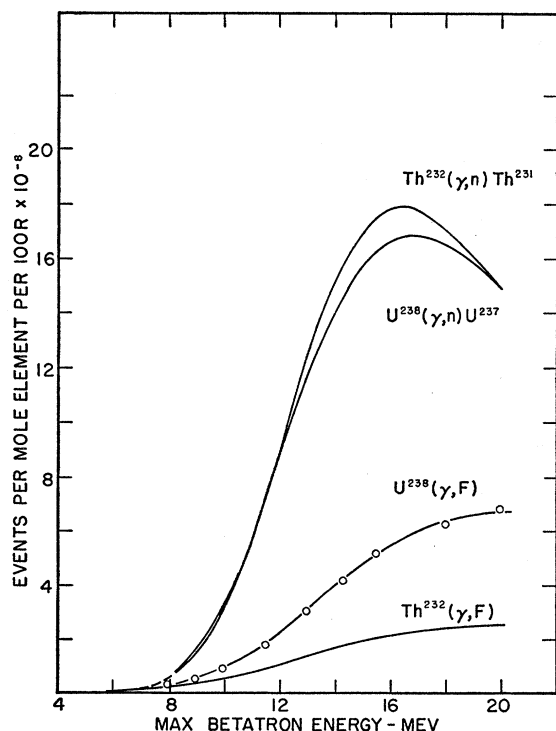


FIG. 3. Activation functions for the photofission and photoneutron reactions in thorium and uranium. \circ , absolute number of uranium photofissions (γ, F) per mole of uranium per 100 r determined in this work. $Th^{232}(\gamma, F)$, $Th^{232}(\gamma, n)Th^{231}$, and $U^{238}(\gamma, n)U^{237}$ activation functions have been normalized against the $U^{238}(\gamma, F)$ absolute activation function. All four activation functions were smoothly extrapolated from 8 to 5 Mev.

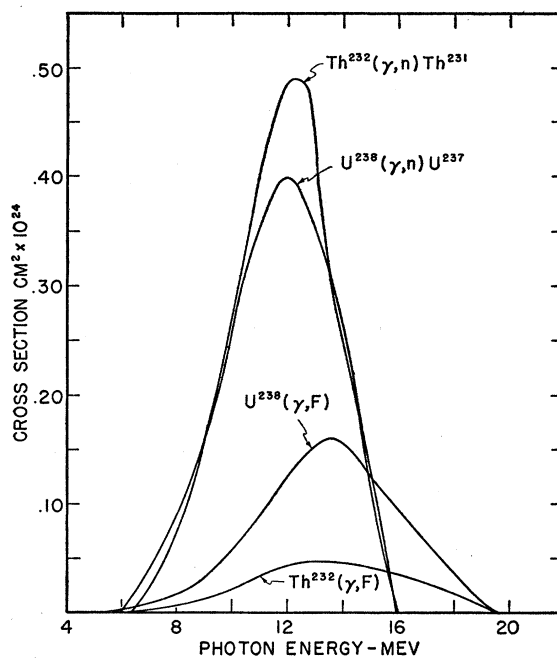


FIG. 4. Photoneutron and photofission cross sections of Th^{232} and U^{238} obtained from analyses of the corresponding activation functions of Fig. 3 by the photon difference method.

III. RESULTS

The experimental results are shown graphically in Figs. 1, 2, and 3. Figure 1 represents the ratio of the (γ, F) yield to the (γ, n) yield per mole of elements, thorium and uranium. The uranium (γ, F) to (γ, n) ratios obtained by Duffield and Huizenga⁴ are shown for comparison. The broken open circles represent data having errors of approximately $\pm 40\%$ because of very low net counting rates in the determination of the number of U^{237} atoms formed; the broken triangle represents an error of $\pm 25\%$ in weighing which affects the determination of the thorium fission yield. In general, the (γ, n) and fission product yields for betatron energies greater than 11 Mev may be considered accurate within 10% and 6%, respectively. For lower betatron energies, these limits tend to increase. Furthermore, since the absolute fission yields were calculated by assuming that the ratio of the Ba^{139} photofission yields in Th^{232} and U^{238} to the Ba^{139} yields in U^{235} slow-neutron fission is 0.9, the absolute fission yields and any ratios in which fission yields appear are correct only in so far as this assumption is correct.

The photofission ratios and the single neutron emission ratios of thorium to uranium are shown as a function of betatron energy in Fig. 2. Again, the broken circles represent values for which very low net counting rates were obtained for the U^{237} yield. Although the ratios of the (γ, n) emission in thorium to uranium define a maximum near 17 Mev, a ratio of unity from 8 to 20 Mev is compatible with the present data.

TABLE III. Excitation function characteristics.

Reaction	σ_{\max} (barns)	$E(\sigma_{\max})$ (Mev)	Half-width (Mev)	$\int \sigma dE^a$ (Mev-barns)
$U^{238}(\gamma, F)$	0.160	13.7	5.8	1.0
$Th^{232}(\gamma, F)$	0.045	13.5	7.7	0.35
$U^{238}(\gamma, n)U^{237}$	0.400	12.0	5.0	2.1
$Th^{232}(\gamma, n)Th^{231}$	0.490	12.2	4.2	2.2

^a Integration limits are 0 to 20 Mev.

The activation functions for the different photo-nuclear reactions are given in Fig. 3. The experimentally measured $U(\gamma, F)$ yields are shown as part of the plot. A small contribution (1 to 2%) of U^{235} to the uranium photofission yield has been neglected in assigning the yields to U^{238} . The other activation functions were calculated using the uranium photofission function and the smoothed ratios of Figs. 1 and 2.

The yield-energy relationships of Fig. 3 have been analyzed by the photon difference method¹⁸ to give cross sections as functions of discrete photon energy. These excitation functions are shown in Fig. 4. The shapes of these cross sections are very sensitive to variations in the activation functions and should not be taken too literally, particularly at the higher energies. Characteristics of these excitation functions are given in Table III for comparison with those in Table I.

Table IV, which is based on excitation functions of Fig. 4, gives the photofission branching ratio, $\sigma_{(\gamma, f)}/[\sigma_{(\gamma, f)} + \sigma_{(\gamma, n)}]$, for photon energies of 8 to 11 Mev.

IV. DISCUSSION

The variation of the (γ, F) to (γ, n) ratios shown in Fig. 1 can be reasonably explained upon the basis of the threshold energies for the different reactions. Thresholds for the various nuclear reactions in which neutron emission and/or fission are involved are given in Table V for the two nuclides, Th^{232} and U^{238} . These thresholds are the result of experimental measurements^{3, 15, 21, 22} and neutron binding energies calculated from closed energy cycles.²³ Since the photofission threshold has been reported to be about 5.1 Mev for U^{238} and the (γ, n) threshold about 6.0 Mev, the (γ, F) to (γ, n) ratio should be infinite for betatron energies

TABLE IV. Photofission branching ratio.

E (Mev)	Th^{232}	Branching ratio	U^{238}
8	0.10		0.21
9	0.08		0.17
10	0.08		0.18
11	0.08		0.20

²¹ Koch, McElhinney, and Gasteiger, Phys. Rev. **77**, 329 (1950).
²² Huizenga, Magnusson, Fields, Studier, and Duffield, Phys. Rev. **82**, 561 (1951).

²³ J. R. Huizenga, Physica **21**, 410 (1955).

between these threshold limits. The fact that the uranium ratio curve does not drop precipitously from an infinite value at 6 Mev can be attributed to the bremsstrahlung spectrum. This spectrum tends to "smear out" sharp energy-dependent effects. The increase of the (γ, F) to (γ, n) ratio beyond 12 Mev is caused by the onset of the (γ, nf) and $(\gamma, 2n)$ reactions. Either process tends to increase the observed ratio of the number of fissions to the number of residual (γ, n) atoms. The ratios of (γ, F) to (γ, n) for thorium define the same general shape as that for uranium and can be explained in a similar manner.

The ratios of the (γ, n) yields of Fig. 2 indicate that, for betatron energies of 10 to 20 Mev, single neutron emission in thorium and uranium occurs with approximately equal probability. Since the (γ, n) threshold for Th^{232} is greater than that for U^{238} by ~ 0.4 Mev, one would expect the Th^{231} to U^{237} ratio to decrease and approach zero as the betatron energy is decreased toward the $Th^{232}(\gamma, n)$ threshold. This expectation is fulfilled as shown in Fig. 5. The relative (γ, n) yields of thorium to uranium indicated by the squares in Fig. 5

TABLE V. Thresholds of neutron-emitting reactions for Th^{232} and U^{238} , ^a

Nuclide	Reaction					
	(γ, f)	(γ, nf)	$(\gamma, 2nf)$	(γ, n)	$(\gamma, 2n)$	$(\gamma, 3n)$
Th^{232}	5.4 ^b	11.8	16.8	6.4 ^d	11.4	18.1
U^{238}	5.1 ^{b, c}	11.2	16.6	6.0 ^e	11.4	17.8

^a Where a particular reference has not been given, the threshold value has been calculated by using experimental data and the difference in binding energies from the tables of reference 23.

^b See reference 21.

^c See reference 3.

^d See reference 15.

^e See reference 22.

have been calculated from the total neutron yields and the mean number of total neutrons per fission of reference 6, assuming reasonable values of $\bar{\nu}$.

Since the photofission threshold of U^{238} is less than that of Th^{232} , one would expect the relative probability of thorium to uranium fission to decrease with decreasing betatron energy, as it does for single neutron emission. This is not indicated, however, by the relative fission probability curve of Fig. 2. This curve shows that thorium fissions more favorably in comparison with uranium as the energy is lowered. Figure 6 represents a compilation of other data from which the relative photofissionability of thorium to uranium has been determined.²⁴⁻²⁸ In this figure, the data of reference 25 have been normalized at 20 Mev to the data of this paper.

The techniques used in evaluating the relative fission probabilities shown in Fig. 6 were varied.

²⁴ J. McElhinney and W. E. Ogle, Phys. Rev. **81**, 342 (1951).

²⁵ R. B. Duffield and J. E. Gindler (unpublished).

²⁶ Huizenga, Gindler, and Duffield, Phys. Rev. **95**, 1009 (1954).

²⁷ R. A. Schmitt and R. B. Duffield (to be published).

²⁸ E. J. Winhold and I. Halpern, Phys. Rev. **103**, 990 (1956).

Measurement of the beta activity of fission fragments captured in metallic foils was used in references 24, 25, and 28; isolation and counting Sr⁹¹, I¹³⁴, and Ba¹³⁹ fission products was used in reference 27; and scintillation counting of fission fragments was used in reference 26. The latter technique involved counting fragments at right angles to the fissile target. For betatron energies less than 16 Mev, it has been shown that the angular anisotropy of the fission fragments of Th²³² and U²³⁸ becomes appreciable.²⁸⁻³¹ Consequently, the 11-Mev ratio of reference 26 has been corrected for the difference at 90° in anisotropies of Th²³² and U²³⁸.

Although the magnitude of the fissionability of thorium relative to that of uranium does not agree completely with that of other workers, Fig. 6 confirms the fact that thorium does show an increased fissionability with respect to uranium as the maximum exciting energy is decreased from about 12 to 8 Mev. For lower energies the fission ratio of thorium to uranium drops rather rapidly. This is consistent with thorium to uranium photofission ratios of about 0.5 obtained with 6.1-Mev gamma rays from the

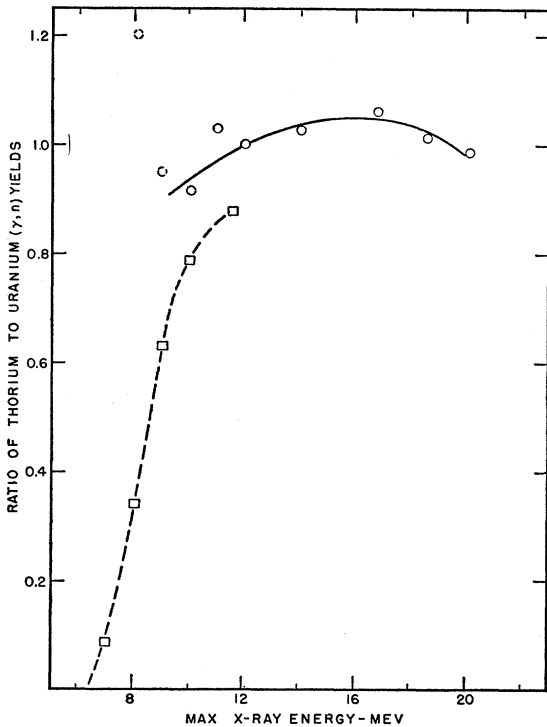


FIG. 5. Ratios of thorium to uranium photoneutron yields as a function of maximum excitation energy. O, ratio of Th²³²(γ,n)Th²³¹ events per mole of thorium per 100 r to U²³⁸(γ,n)U²³⁷ events per mole per 100 r of this work; □, same ratio of Th²³²(γ,n)Th²³¹ to U²³⁸(γ,n)U²³⁷ calculated from ratios of [Th²³²(γ,N) - $\bar{\nu}$ · Th²³²(γ,F)] ÷ [U²³⁸(γ,N) - $\bar{\nu}$ · U²³⁸(γ,F)] taken from reference 6.

²⁹ Winhold, Demos, and Halpern, Phys. Rev. **85**, 728 (1952).

³⁰ Winhold, Demos, and Halpern, Phys. Rev. **87**, 1139 (1952).

³¹ Fairhall, Halpern, and Winhold, Phys. Rev. **94**, 733 (1954).

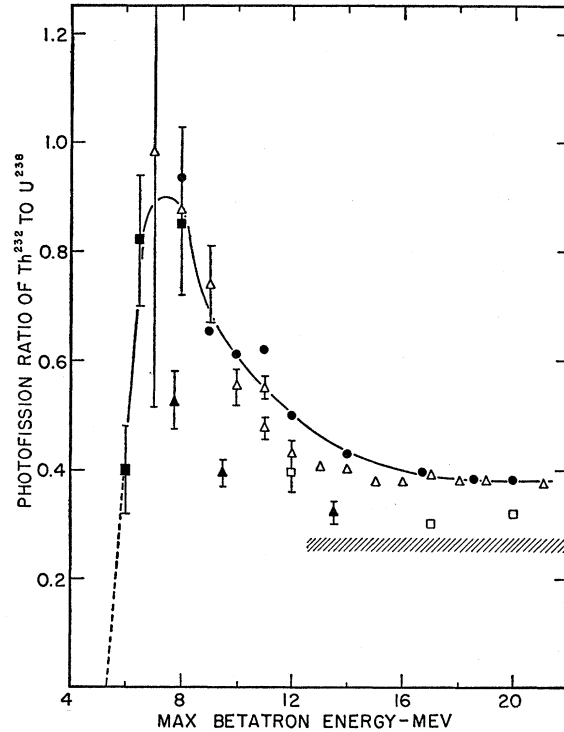


FIG. 6. Thorium to uranium fissionability ratio as a function of maximum excitation energy. ●, this paper; //, reference 24; Δ, reference 25 (data normalized to present data at 20 Mev); □, reference 26; ■, reference 27; ▲, reference 28.

F¹⁹($p,\alpha\gamma$)O¹⁶ reaction^{32,33} and the fact that the Th²³² photofission threshold is approximately 0.3 Mev greater than that of U²³⁸.

Since the observed anisotropy²⁸⁻³¹ in the photofission of even-even nuclides has been explained³⁴ in terms of the fissioning nuclei passing through the saddle point in the (1-) collective excitation state, it is of interest to compare the low energy fissionability of Th²³² and U²³⁸ with the energies of their respective first collective (1-) excitations at the saddle point. Information gained from alpha decay studies on the energy of the collective (1-) excitations of the ground state indicates, however, that this energy increases with increasing Z above thorium.³⁵ Bohr³⁴ has suggested that for excitation energies slightly above the fission threshold, the rotational excited states will be similar to the observed low-energy excitations of the nuclear ground state since most of the total energy is bound in potential energy of deformation. A lower energy for the first (1-) state

³² Haxby, Shoupp, Stephens, and Wells, Phys. Rev. **59**, 57 (1941).

³³ W. H. Hartley, Ph. D. thesis, University of Pennsylvania, 1955 (unpublished); Proceedings of the Photonuclear Conference at Case Institute of Technology, 1955 (unpublished), pp. 2-3.

³⁴ A. Bohr, Proceedings of the International Conference on the Peaceful Uses of Atomic Energy, August 8-20, 1955, Physics; Research Reactors (United Nations, New York, 1956), Vol. 2, p. 151.

³⁵ Stephens, Asaro, and Perlman, Phys. Rev. **100**, 1543 (1955).

above fission threshold for Th^{232} would be consistent with the experimental evidence that Th^{232} becomes more fissionable relative to U^{238} as the maximum betatron energy is reduced from 12 to 8 Mev.

Competition between fission and neutron emission probably affords the most likely explanation of the relative fissionability curve of Fig. 6. Since uranium requires a lower energy to fission than thorium, the thorium to uranium fission ratio is zero at the thorium (γ, f) threshold. However, since neutron emission can complete with fission at a lower energy in uranium than in thorium, uranium nuclei excited with energies between the (γ, n) thresholds of U^{238} and Th^{232} will preferentially de-excite by neutron emission, whereas thorium nuclei excited with these energies will fission. Consequently, thorium fission should increase with respect to uranium fission. Once the thorium (γ, n) threshold (6.4 Mev) is reached, neutron emission competes with fission. Since the uranium fission branching ratio appears to be at least twice as large as that for thorium (Table IV), one would expect the relative fissionability ratio of thorium to uranium to decrease with increasing excitation energy. However, the combination of the shape of the bremsstrahlung spectrum and the (γ, f) and (γ, n) cross sections below 6.4 Mev are apparently responsible for the near constancy of the fissionability ratio from ~ 6.5 to ~ 8.5 Mev betatron energy. The leveling off of the fission ratio beginning at ~ 14 Mev in Fig. 6 is consistent with the idea that a given nuclide fissions with a particular probability²⁶ over the energy region in which the giant photonuclear absorption resonance occurs, and that lower energy effects do not alter this probability to any great extent.

It is of interest to note that if one extrapolates the fission ratio of Fig. 6 to zero at the thorium photofission threshold and then attempts to derive differential cross sections for both thorium and uranium that satisfy the smooth curve from 5 to 8 Mev, one concludes that either the photofission cross section of thorium or uranium or both has a small bump, resembling a resonance, near the (γ, n) thresholds for the respective nuclides. Such a bump has also been reported by Winhold and Halpern²⁸ for the photofission cross sections of Th^{232} and U^{238} but not for U^{235} . Also, bumps have been found²⁷ at approximately 6.5 Mev for the asymmetric and symmetric photofission of U^{238} and in the asymmetric photofission of Th^{232} . No bump was found in the symmetric photofission of Th^{232} . (These cross sections were determined by analyzing appropriate fission product yields by means of the photon difference method.) The appearance of these bumps in the total (asymmetric plus symmetric) photofission cross sections of Th^{232} and U^{238} is consistent with the idea of the successful competition of neutron emission with fission at, or slightly above, the (γ, n) threshold. The absence of such a bump in the U^{235} photofission

cross section is also consistent, since its (γ, n) threshold is ~ 0.2 Mev less than the (γ, f) threshold.

Any anomalous effects such as bumps in the fission cross section that occur about 1 Mev above the fission thresholds do not appreciably change the shapes of the curves and the corresponding integrated cross sections from threshold to 20 Mev. Consequently, the cross sections shown in Fig. 4 and their corresponding characteristics found in Table III have been averaged over any bumps found in the energy region from threshold to 8 Mev.

A comparison of the uranium excitation function characteristics of both (γ, F) and (γ, n) (see Tables I and III) shows favorable agreement with previous studies of references 4 and 5. By subtracting the thorium and uranium photofission integrated cross sections, $\int_0^{20} \sigma(\gamma, F) dE$, of this work (Table III) from the corresponding thorium and uranium photofission integrated cross sections, $\int_{20}^{28} \sigma(\gamma, F) dE$, of reference 6, it is calculated that $\int_{20}^{28} \sigma(\gamma, F) dE$ for thorium and uranium are 0.29 and 0.71 Mev barn, respectively. The calculated uranium (γ, F) difference of 0.71 Mev-barn in the 20- to 28-Mev range is higher than other data^{5,17} would warrant by at least a factor of three, while the paucity of thorium data precludes any direct comparisons.

By comparing the thorium and uranium photofission branching ratios of this work (Table IV) and that of reference 6 (Table II), it is felt that the average number of neutrons emitted per thorium and uranium photofission for absorption of 8- to 11-Mev photons is ≤ 2.5 . A loss of 2.0 ± 0.5 neutrons per fission act is compatible with the fission of thorium³⁶ and uranium³⁷ induced by fission-spectrum neutrons.

We have attempted to determine the shapes and magnitudes of the $(\gamma, 2n)$ excitation functions for Th^{232} and U^{238} by combining the data of this paper with those of reference 6. This reference gives the cross section for total neutron emission for the two nuclides, Th^{232} and U^{238} , as functions of photon energy from 0 to 28 Mev. Since charged particle emission is small for these nuclides compared to fission and neutron emission,⁹⁻¹² the total neutron cross section for excitation energies of 18 Mev or less becomes $\sigma(\gamma, N) = \sigma(\gamma, n) + 2\sigma(\gamma, 2n) + \bar{\nu}\sigma(\gamma, F)$. Consequently, the $(\gamma, 2n)$ cross sections depend greatly upon the values of $\bar{\nu}$ used in the calculation. This is particularly true for uranium, since its photofission cross section represents a larger portion of the total photonuclear absorption cross section than the corresponding cross section of thorium. For our calculations we have assumed $\bar{\nu}$ to vary uniformly from about 2 for photons of 6 Mev to 5 for photons of 18 Mev.

Results of the $(\gamma, 2n)$ cross section calculations are: $E_{\sigma_{\max}}$ was found to be between 15 and 16 Mev for both thorium and uranium; the half-widths varied from 2.5

³⁶ A. Turkevich and J. B. Niday, Phys. Rev. **84**, 52 (1951).

³⁷ Keller, Steinberg, and Glendenin, Phys. Rev. **94**, 969 (1954).

to 4 Mev for both nuclides; the integrated cross section from 0 to 20 Mev varied from 0.7 to 1.4 Mev barns for thorium and 0.3 to 1.1 Mev barns for uranium. Since (1) the integrated photonuclear absorption cross section should be approximately the same for the two nuclides, (2) the integrated (γ, n) cross sections are nearly identical, and (3) the integrated photofission cross section for U^{238} is about three times that for Th^{232} , it is not too surprising that the integrated $(\gamma, 2n)$ cross section appears to be larger for Th^{232} than for U^{238} .

Levinger and Bethe³⁸ and Gell-Mann, Goldberger, and Thirring³⁹ have formulated theoretical expressions for the integrated photonuclear absorption cross section which depend upon the neutron number N , proton number Z , and mass number A . Levinger and Bethe⁴⁰ have shown that the 320-Mev photoneutron yields for Cu, I, Ta, Bi, and U (for which a photofission branching ratio of 0.23 is assumed) are in agreement with the formula

$$\int_0^{\infty} \sigma dE = 0.14NZ/A.$$

This formula indicates integrated cross sections of 7.7 and 7.9 Mev-barns for Th^{232} and U^{238} , respectively. Eyges⁴¹ has shown that, on the basis of data for Sb, Ta, and Pb, the above formula predicts values which are approximately 1.7 times too large for the low-energy region (less than 20 Mev). This would indicate the

³⁸ J. S. Levinger and H. A. Bethe, Phys. Rev. **78**, 115 (1950).

³⁹ Gell-Mann, Goldberger, and Thirring, Phys. Rev. **95**, 1612 (1954).

⁴⁰ J. S. Levinger and H. A. Bethe, Phys. Rev. **85**, 577 (1952).

⁴¹ L. Eyges, Phys. Rev. **86**, 325 (1952).

respective integrated cross sections for Th^{232} and U^{238} to be 4.6 and 4.7 Mev-barns over the energy region with which we are concerned. These latter values are in agreement with values of 4.7 and 4.8 Mev barns obtained from the Gell-Mann, Goldberger, and Thirring formula,

$$\int_0^{\mu} \sigma dE = 0.060(ZN/A)[1 + 0.1A^2/NZ],$$

where μ is the mesonic threshold.

Assuming average values of 1.0 and 0.7 Mev-barn for the integrated $(\gamma, 2n)$ cross sections of Th^{232} and U^{238} , respectively, we find that the sums of the integrated (γ, F) , (γ, n) , and $(\gamma, 2n)$ cross sections from 0 to 20 Mev are 3.6 and 3.8 Mev barns for the two respective nuclides. From the integrated cross sections calculated above, approximately 1 Mev barn of the photonuclear absorption cross section would be attributable to gamma-ray scattering and/or higher order particle emission. This appears to be consistent with gamma scattering data⁴² and high-energy neutron production data.⁷

ACKNOWLEDGMENTS

We wish to express our appreciation to Professor R. B. Duffield for helpful discussions. We also wish to thank Mr. T. J. Keegan and members of the University of Illinois 22-Mev betatron operating crew who made the experimentation possible. The technical assistance of Miss M. Petheram, Mr. R. F. Barnes, and members of the Analytical Chemistry Group of Argonne National Laboratory has been greatly appreciated.

⁴² J. Goldemberg and L. Katz, Phys. Rev. **90**, 308 (1953).